City Research Online

City, University of London Institutional Repository

Citation: Hayes, M. J., Tracey-White, D., Kam, J. H., Powner, M. B. & Jeffery, G. (2021). The 3D organisation of mitochondria in primate photoreceptors. Scientific Reports, 11(1), 18863. doi: 10.1038/s41598-021-98409-7

This is the published version of the paper.

This version of the publication may differ from the final published version.

Permanent repository link: https://openaccess.city.ac.uk/id/eprint/26881/

Link to published version: https://doi.org/10.1038/s41598-021-98409-7

Copyright: City Research Online aims to make research outputs of City, University of London available to a wider audience. Copyright and Moral Rights remain with the author(s) and/or copyright holders. URLs from City Research Online may be freely distributed and linked to.

Reuse: Copies of full items can be used for personal research or study, educational, or not-for-profit purposes without prior permission or charge. Provided that the authors, title and full bibliographic details are credited, a hyperlink and/or URL is given for the original metadata page and the content is not changed in any way.

City Research Online: http://openaccess.city.ac.uk/ publications@city.ac.uk

scientific reports

Check for updates

OPEN

The 3D organisation of mitochondria in primate photoreceptors

Matthew J. Hayes[1]✉, Dhani Tracey-White[1], Jaimie Hoh Kam[1], Michael B. Powner[2] & Glen Jeffery[1]

Vertebrate photoreceptors contain large numbers of closely-packed mitochondria which sustain the high metabolic demands of these cells. These mitochondria populations are dynamic and undergo fusion and fission events. This activity serves to maintain the population in a healthy state. In the event of mitochondrial damage, sub-domains, or indeed whole mitochondria, can be degraded and population homeostasis achieved. If this process is overwhelmed cell death may result. Death of photoreceptors contributes to loss of vision in aging individuals and is associated with many eye diseases. In this study we used serial block face scanning electron microscopy of adult *Macaca fascicularis* retinae to examine the 3D structure of mitochondria in rod and cone photoreceptors. We show that healthy-looking photoreceptors contain mitochondria exhibiting a range of shapes which are associated with different regions of the cell. In some photoreceptors we observe mitochondrial swelling and other changes often associated with cellular stress. In rods and cones that appear stressed we identify elongated domains of mitochondria with densely-packed normal cristae associated with photoreceptor ciliary rootlet bundles. We observe mitochondrial fission and mitochondrion fragments localised to these domains. Swollen mitochondria with few intact cristae are located towards the periphery of the photoreceptor inner-segment in rods, whilst they are found throughout the cell in cones. Swollen mitochondria exhibit sites on the mitochondrial inner membrane which have undergone complex invagination resulting in membranous, electron-dense aggregates. Membrane contact occurs between the mitochondrion and the photoreceptor plasma membrane in the vicinity of these aggregates, and a series of subsequent membrane fusions results in expulsion of the mitochondrial aggregate from the photoreceptor. These events are primarily associated with rods. The potential fate of this purged material and consequences of its clearance by retinal pigment epithelia are discussed.

Photoreceptors represent most of the energy consumption of the retina[1,2]. They require ATP for the transport of ions during the depolarisation and hyperpolarisation currents of phototransduction (particularly the Na^+/K^+ ATPase[3,4] during the dark current), and for lipid and protein synthesis that is required for outer segment renewal as 10% of the distal tip of the outer segment is replaced every day. More than 80% of glucose taken up by the photoreceptor is used for anaerobic glycolysis[5], but a proportion of ATP is provided by mitochondria[2]. Mitochondria are also vital in the compartmentation of cell metabolism and regulation of programmed cell death[6].

Photoreceptors are highly polarised, terminally differentiated cells and in most vertebrate species mitochondria are predominantly packed into a region of the inner segment called the *ellipsoid*.

Photoreceptors are bathed in incident radiation and exposed to reactive oxygen and nitrogen species (RONS) generated by mitochondria and by the ionising effects of light on photosensitizing molecules such as retinoids. Oxidation of abundant long-chain polyunsaturated fatty acids (PUFAs) produces highly-reactive electrophilic intermediates that generate free-radicals. Hence, photoreceptor mitochondria accumulate damaging modifications through thermal, photoreaction and redox mechanisms[7,8]. Mitochondria may then signal cell death by a number of programmed mechanisms including apoptosis[9]. In primates, including humans, up to 30% of rods are lost over life, but there is little evidence for cell death in the cone population, although these suffer functional decline[10].

Mitochondrial populations in cells are heterogeneous, their morphology changing in response to damage, stress or metabolic demand. Mitochondrial biogenesis occurs as a result of fission[6]. By growing new mitochondria

[1]University College London Institute of Ophthalmology, 15-43 Bath Street, London EC1V 9EL, UK. [2]City, University of London, Northampton Square, London EC1V 0HB, UK. ✉email: M.Hayes@ucl.ac.uk

from the best elements of existing ones, the cell avoids accumulating errors. Homeostasis occurs by highly-regulated interplay between fission, fusion and autophagy[6,11–18]. In mammalian cells, mitochondrial fusion is performed by mitofusin-1, mitofusin-2 (MFN-1/2) and optic atrophy-1 (OPA1). By sharing and mixing their contents dysfunctional mitochondria are thought to mitigate localised damage[19]. Here we generate 3D reconstructions from serial sections of mitochondria in healthy-looking and apparently stressed rods and cones to see if there are intracellular, localised variations in morphology that are likely to reflect dynamic homeostasis.

In photoreceptors a ciliary rootlet extends from the pair of basal bodies at the base of the cilium. In transmission electron microscope longitudinal sections, it appears striated, the banding representing overlapping components of the intermediate filament rootletin[20]. The rootlet is inherently 'non-directional' being composed of symmetrically arranged elements having no positive or negative end. It is thought unlikely that it could be used for directional trafficking of cell components. In mice it is relatively short, extending as far as the Golgi region of the inner segment and is thought to be associated with Golgi-derived vesicular structures. In primates it is much longer, and is often branched. It extends along the length of the cell, around the nucleus and as far as the synaptic termini. In mutant mice deficient for rootletin, the outer segment forms as normal, but soon degenerates, suggesting that the rootlet is involved in maintenance or stabilisation of the outer-segment; though it is not known how the rootlet accomplishes this and it is not known if it has any similar function in primates[21].

Mitochondria have been shown to associate with the photoreceptor rootlet in owl monkey and bovine retinae[22,23]. As the rootlet is so large in primates and runs directly through the mitochondrial ellipsoid we wondered if it contributes to organisation and homeostasis of the mitochondria. Owl monkeys are nocturnal new world monkeys, so we were interested to see if mitochondria associated with the rootlet in the diurnal old world primate *Macaca fascicularis*. We show that a proportion of mitochondria, those densely furnished with cristae, and exhibiting a narrow diameter, do associate with the rootlet. We identify mitochondrial fission events localised to this region. We also describe a process by which membranous, electron-dense domains of the inner mitochondrial membrane in swollen mitochondria are expelled from photoreceptors. These results suggest photoreceptor mitochondria homeostasis is a cycle of fission associated with the rootlet and piecemeal degradation and expulsion through the plasma-membrane.

Methods

Animals: primates. Ocular tissues were acquired from a large, long-established colony of *Macaca fascicularis* maintained by Public Health England regulated under local and U.K. Home Office regulation. The primary purpose of animal usage was different from the aims of this study and primarily concerned with reducing colony size. Eyes were only retrieved after death. This was identical to Hoh Kam et al. 2019 (Scientific Reports 9:12574[24]). Hence no experiments were undertaken as tissues were harvested after death which is not a regulated procedure. All animals were heathy and were sacrificed by their owners at Public Health England between 9 and 11 a.m. Animals were sedated with 200 mg/kg of Ketamine I/M and then terminally anaesthetised with 2.5 ml of Nembutal (50 mg sodium pentobarbital per mg) delivered to the heart. Eyes were removed at the point of death and were fixed overnight in cold Karnovsky's fixative (2% paraformaldehyde, 2.5% glutaraldehyde in 0.08 M cacodylate buffer). All experimental protocols were approved by The Home Office UK and by the local ethics committee of Public Health England and were in accordance with relevant guidelines and regulations and ARRIVE guidelines. Primates were of Mauritian origin and have a smaller gene pool than those from Indonesia and age more rapidly. Their normal maximum lifespan is around 18 years in this colony. In all experiments retinal tissue from at least five individuals between 12 and 18 years of age was examined.

Conventional transmission electron microscopy. Small portions of the perifoveal retina were dissected from fixed eyes. They were washed 3 times in phosphate buffer and osmicated with 1% osmium tetroxide in ddH_2O for 1 h. Samples were then washed 3×10 min in ddH_2O and dehydrated with a series of ethanol dilutions: 30%, 50%, 70%, 90%, $3 \times 100\%$ and $2 \times$ propylene oxide (at least 20 min in each). They were infiltrated with 50:50 propylene oxide:araldite resin overnight and with several changes of 100% resin the next day. Blocks were cured at 60 °C overnight. Sectioning was performed using a Leica Ultracut UCT microtome. Sections were counter-stained with Reynold's lead citrate and were viewed on a JEOL 1400 + TEM (JEOLUSA MA, USA).

Serial block face scanning electron microscopy SBF-SEM (after Walton 1979[25]). Specimens were fixed in Karnovsky's EM fixative (as above) for 30 min. They were washed 3 times with phosphate buffer. Samples were incubated for 2 h in 2% osmium tetroxide/1.5% ferricyanide and washed 3×5 min in water. The samples were placed in 1% thiocarbohydrazide solution for 10 min and then washed 3×5 min in water. A second phase of osmication was performed (2% osmium tetroxide (no ferricyanide) for 30 min) and the tissue washed again in water. The samples were then placed in aqueous 2% uranyl acetate overnight at 4°.

The following day samples were placed in freshly made Walton's lead aspartate (pH 5.5) for 30 min in a 60 °C oven and subsequently washed 3×5 min in water. Samples were then dehydrated with ethanol (30%, 50%, 70%, 90%) to $100\% \times 3$ then in acetone 2×20 min. Samples were infiltrated with Durcapan resin 25% plus acetone, then 50%, 75% (2 h each) and left overnight in 100% resin. The following day the resin was exchanged, and the blocks hardened in an oven for 48 h. The samples were examined on a Zeiss Sigma VP SEM fitted with a Gatan 3View system.

Quantitation of mitochondrial distribution. The distance of the mitochondria from the center of the photoreceptor and the diameters of these mitochondria in normal and degenerate photoreceptors was measured from individual transverse transmission electron micrographs using ImageJ. Results are from 5 animals and at least 5 cells in each case. Statistical differences between normal and degenerate and rootlet-associated

and non-associated mitochondria were calculated by two-tailed Mann–Whitney U Tests. *** Implies statistical significance > than P = 0.0001. Un-labelled pairwise comparisons failed to reach significance of P = 0.01 and were considered to be insignificant.

Results

3D structure of healthy-looking cones. In TEM sections of cone photoreceptors mitochondria appear as closely-packed oval structures. Examination of sections at different orientations gives little additional insight into their arrangement and structure. We performed serial block face scanning electron microscopy (SBF-SEM) to allow us to identify individual mitochondria across several hundred such sections and thus reveal their 3D structure and position in the photoreceptor.

Figure 1 shows a 3D reconstruction of every mitochondrion in a cone in the peripheral retina of a 14 year-old animal generated by manual segmentation from an SBF-SEM stack. The ellipsoid contains a densely-packed array of mostly elongated mitochondria arranged broadly parallel to the long axis of the photoreceptor. The cell contained 498 individual mitochondria. The apical mitochondria terminated in narrow tips whilst those that terminated distally were swollen. In this cell we identified few mitochondrial fragments; those present were mostly apical.

Dispersed throughout the cell were a small number of spheroidal mitochondria which had an electron lucent matrix and few cristae. The volume of these mitochondria was found to be greater than those of the denser, elongated mitochondria; indicating they were swollen as well as being of an altered shape (Fig. 2D–G).

In individual TEM sections the mitochondria of large, parafoveal cones appear as closely-packed ovals, in transverse sections mostly as circles (Fig. 2A,B). 3D rendering of these from SBF-SEM stacks reveal them to have a range of morphologies (Fig. 2C–E). Mitochondria closest to the photoreceptor plasma membrane (cortical) exhibited extended membrane contact sites with the plasma membrane. These mitochondria were uniformly narrow and elongated, having a high length/width ratio. Those less closely associated with the plasma membrane (inner mitochondria) had slightly broader, shorter profiles. Those at the distal end were shorter and broader still (Fig. 2F,G).

Mitochondrial fragments were localised to the innermost core of the cell and tended to be more apical than distal (Fig. 2C–E).

3D structure of healthy-looking rods. Figure 3A,B shows a 3D reconstruction of every mitochondrion in a small, healthy-looking rod in the parafoveal region of a 12 year-old individual. The mitochondria are all narrow and elongated (Fig. 3A), have a more restricted range of volumes than is observed in cones (Fig. 3C) and in transverse section (TEM) appear mostly circular (Fig. 3D). In such sections it is possible to identify the ciliary rootlet. Some mitochondria appear to be in close contact with this structure. In the schematic the ciliary rootlet is highlighted in red and rootlet-associated mitochondria in blue.

Mitochondria in stressed cone photoreceptors. As described above, mitochondria in healthy-looking cones appear to have a dense matrix and are rich in cristae. In some cases we observed mitochondrial extensions along the ciliary rootlet (Fig. 4A).

Generally, in apparently stressed cones we saw few atypical, swollen mitochondria or inclusions (consistent with their survival through ageing compared with rods); however, some regions of the adult retina exhibited cones which appeared to be stressed. In some cases these were in very close proximity to dead rods (identified as being highly condensed, with little or no outer segment and having few identifiable remaining organelles). Stressed cells were identified as having swollen or heterogeneous mitochondria but in which the outer segment, nucleus, endoplasmic reticulum and Golgi appeared normal. There was no evidence of overt apoptosis or necrosis (Fig. 4B).

A minority of mitochondria in these cells had empty regions of matrix, few linear cristae and instead contained aggregates of electron-dense deposits surrounded by what appear to be concentric or spirally arranged whorls of membrane (see arrows in Fig. 4B).

Reconstructions from segmentation of SBF-SEM stacks of cones revealed most of these aggregates to be fully internal to the bounding outer mitochondrial membrane (Fig. 4C,D). Under the sample preparation conditions used for SBF-SEM, the contents of the cristae of the mitochondria appear electron-dense and the mitochondrial inter-membrane space is also packed with dense material (though less so than the cristae). The electron-dense inclusions are associated with the mitochondrial periphery. We identify a region of electron-lucid mitochondrial inter-membrane (MIM) space in the vicinity of these inclusions suggesting that the dense components have been drawn into the whorl of membrane (Fig. 5A white arrow).

More than 90% of cones exhibited few obvious mitochondrial morphological changes; but most contained a number of mitochondria containing electron-dense material. Examination of cones from the central retina from five specimens (ages 14–18 years) suggested to us a speculative series of events leading to the mitochondria expelling the electron-dense material through the plasma membrane of the photoreceptor (Fig. 5A–H). The dense aggregate forms in the vicinity of the inter-membrane space and this region of MIM is altered (Fig. 5A,B). In cones this appears stable as we never observe aggregates free in the cytoplasm. If the mitochondrion contacts the photoreceptor plasma membrane, the outer mitochondrial membrane in this altered domain promotes partial membrane rupture or fusion (Fig. 5C,D). Subsequently, the mitochondrial membranes swell out through the rupture in the plasma membrane and are likely expelled into the inter-photoreceptor space (Figs. 4E,F, 5E–H). We presume the plasma membrane and mitochondrial inner and outer membrane reseal and the mitochondrion, now purged of its aggregate, can return to the cell population.

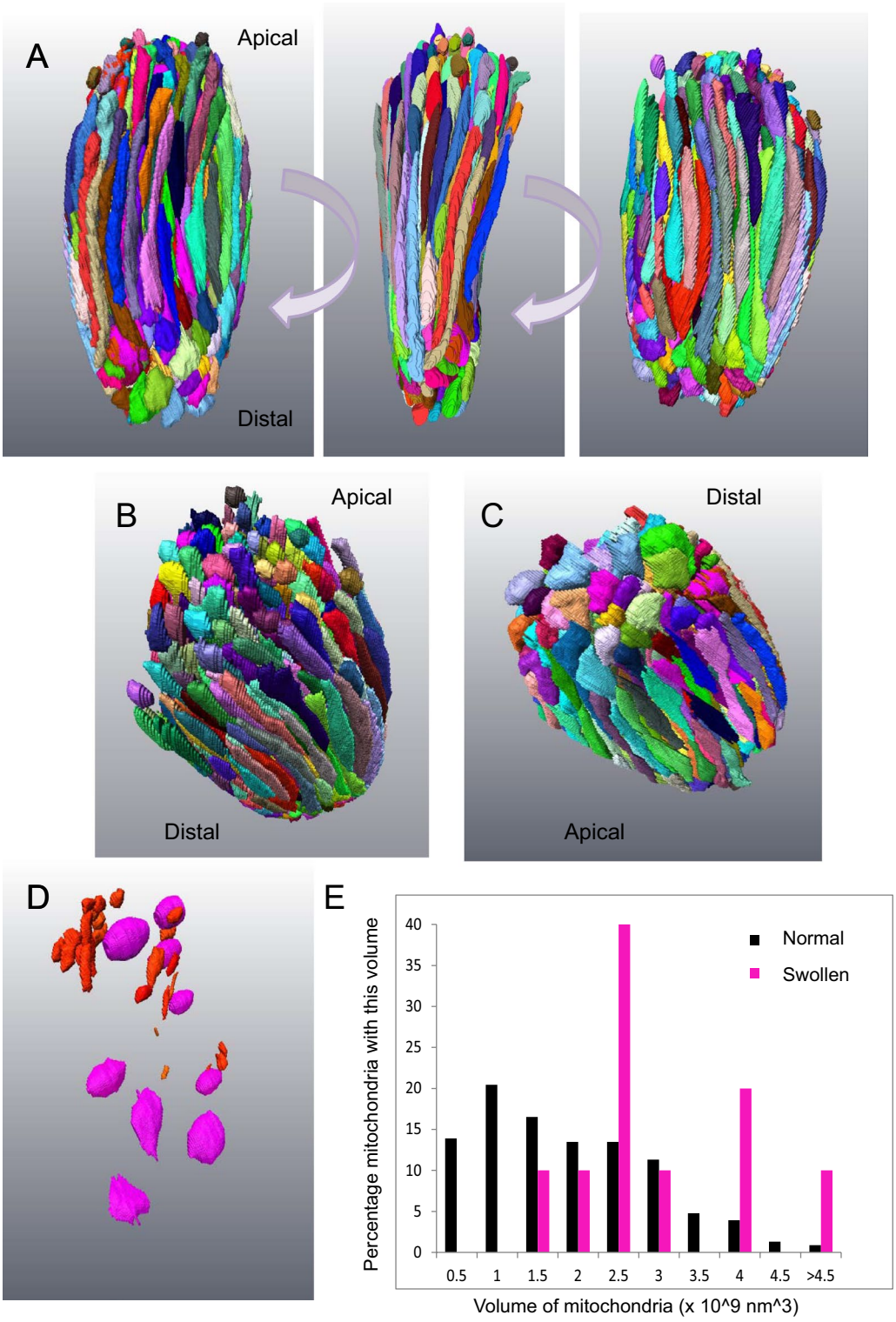

Figure 1. 3D rendering of complete segmentation of every mitochondrion in a small, healthy-looking cone. (**A**) Three panels represent 90 degree rotations of the ellipsoid of a cone cell showing all the mitochondria. The mitochondria show a range of profiles, though most are long and thin. (**B**) Mitochondria at the apical end of the ellipsoid terminate with narrow tips. There were also numerous mitochondrial fragments. (**C**) Those at the distal end were swollen at their tip. (**D**) Mitochondrial fragments (red) are mostly localised to the apical domain of the ellipsoid. Spheroidal, swollen mitochondria (magenta) are found throughout. (**E**) Histogram showing the range of mitochondrial volumes in this ellipsoid. The spheroidal mitochondria (magenta) have a greater average volume.

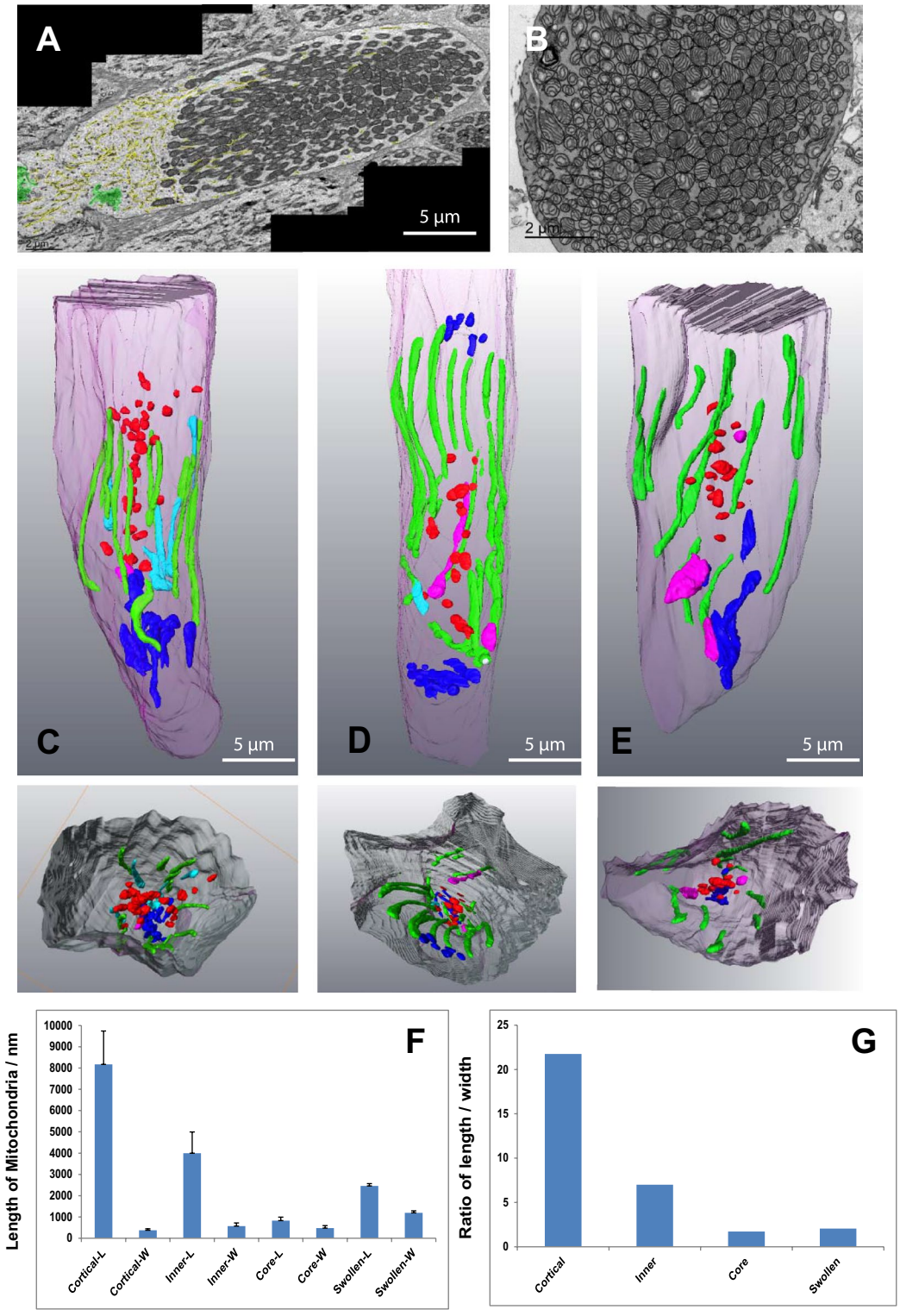

Figure 2. In healthy-looking cones different mitochondrial shapes are associated with different parts of the photoreceptor. (**A**) A montage of several TEM micrographs of the longitudinal section of a healthy-looking cone. The ER is high-lighted in yellow, the Golgi apparatuses in green. (**B**) A TEM micrograph showing a transverse section through a healthy-looking cone. Mitochondria are densely-packed in the ellipsoid. (**C**–**E**) Partial 3D segmentation of 3 representative cones identifying different mitochondrial shapes in different regions of the cone ellipsoid. The smaller panels beneath show cut transverse sections through these constructions. (**F**) Histogram showing the average lengths of mitochondria from different parts of the cone. (**G**) Histogram showing the ratio between length and width of mitochondria from different regions of the cone. Mitochondria intimately associated with the plasma membrane of the cone (green) are elongated. Those *inner* mitochondria that are only partially associated with the plasma membrane (cyan) are shorter and have a more varied width. Mitochondria at the base of the cone are shorter and stubbier (dark blue). Mitochondria fragments in the core of the cone (red) are very small.

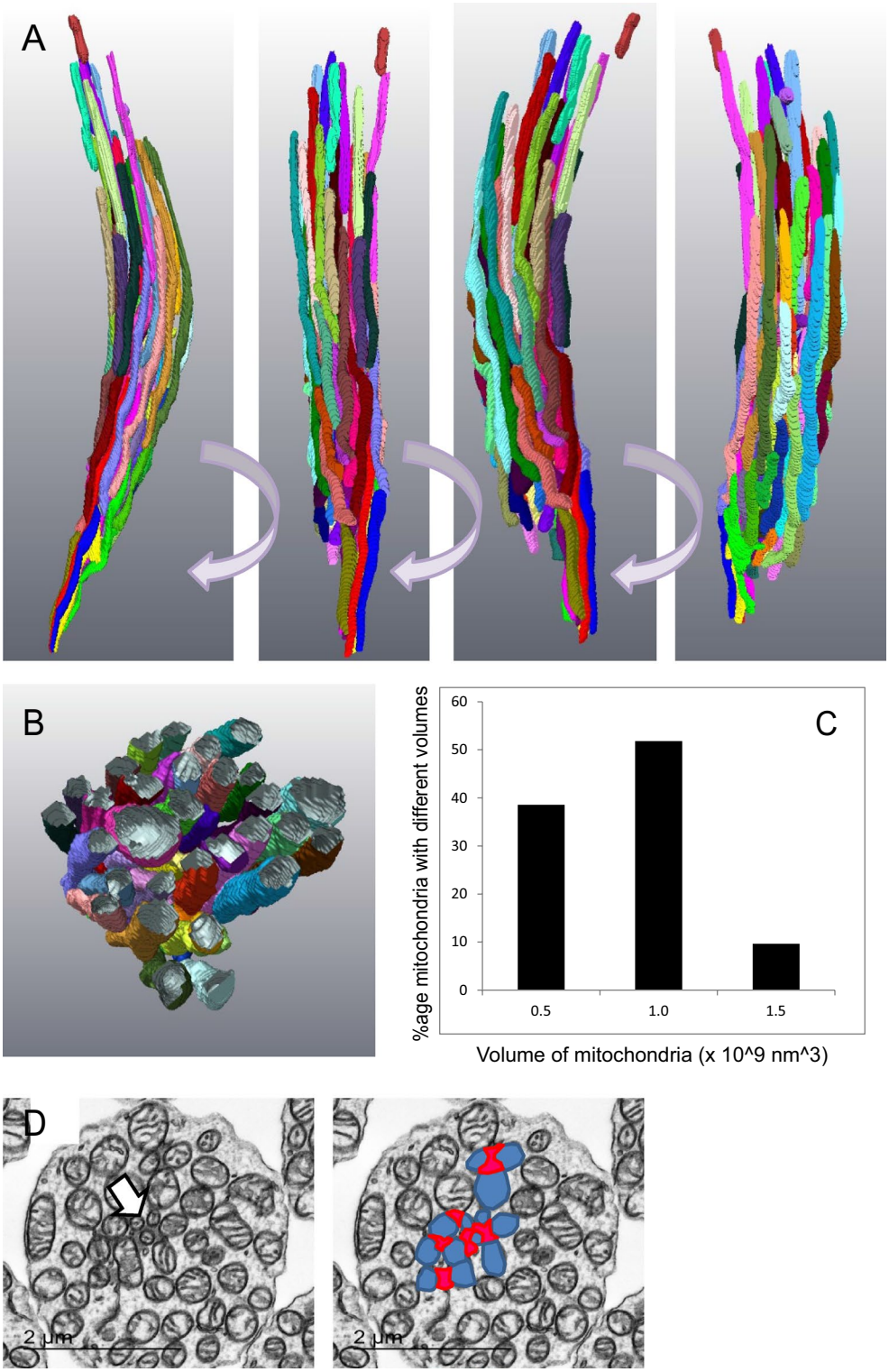

Figure 3. 3D rendering of complete segmentation of every mitochondrion in a healthy-looking rod. (**A**) Rotations of a 3D reconstruction of segmentation of mitochondria in a normal, healthy-looking rod. All the mitochondria are elongated and aligned along the long axis of the rod. (**B**) Transverse section generated from the 3D reconstruction. (**C**) Distribution of mitochondria volumes. (**D**) Transverse section showing the position of the rootlet and its association with mitochondria (high-lighted in the next panel); ciliary rootlet in red, associated mitochondria in blue.

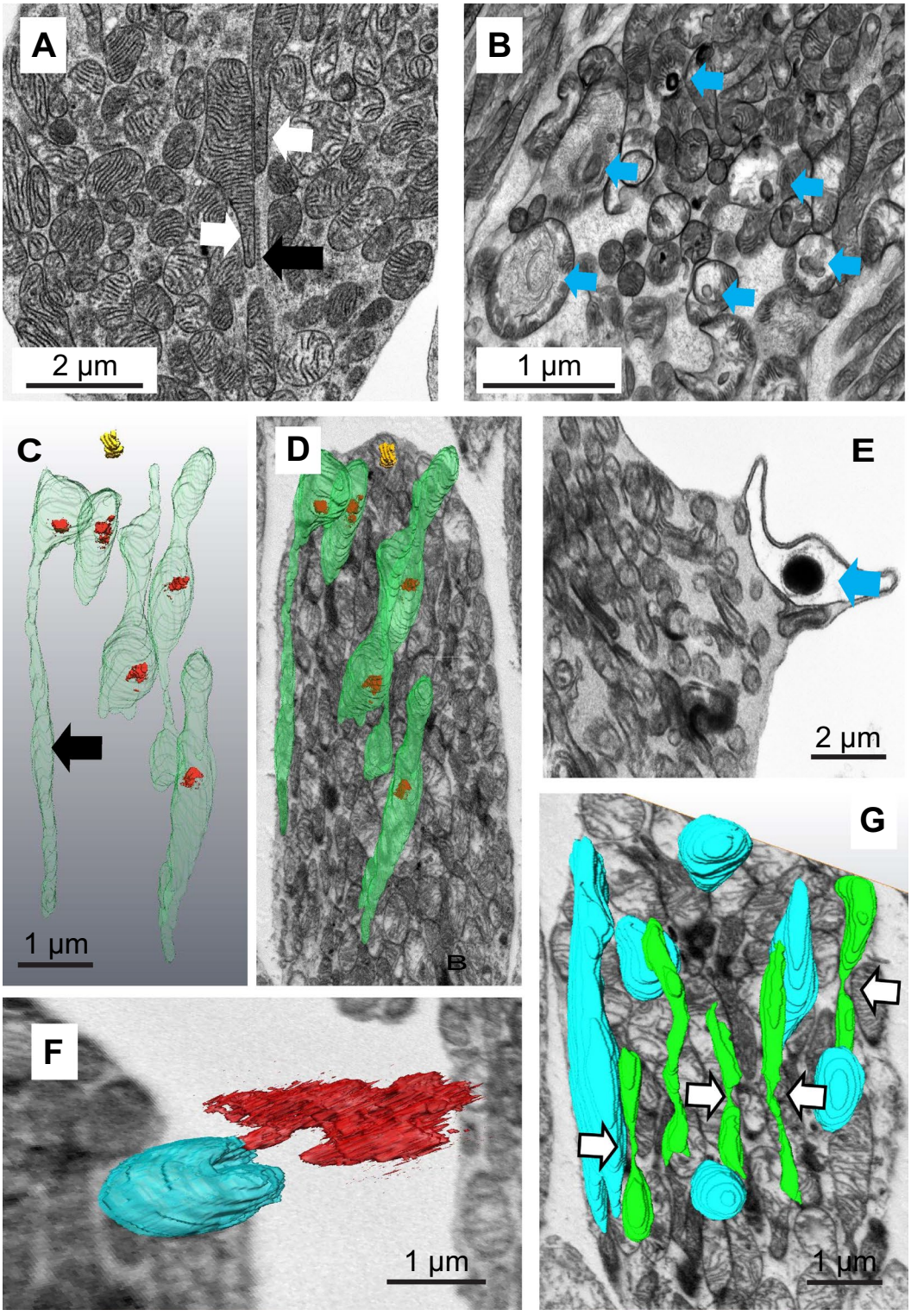

Figure 4. Mitochondria in stressed cones. (**A**) Oblique section through a healthy-looking cone showing two mitochondria with extensions (white arrows) associated with the ciliary rootlet (black arrow). (**B**) Oblique section through a stressed cone illustrating a range of mitochondria forms (mitochondria containing few cristae and electron-dense aggregates marked with a blue arrow). (**C**) 3D reconstruction of mitochondria containing electron dense inclusions (**D**) Super-position of this reconstruction on a single SBF-SEM section showing their position in the cell. (**E**) A swollen mitochondrion containing an electron-dense inclusion associated with the plasma membrane. (**F**) A 3D reconstruction from a SBF-SEM stack showing a C-shaped, plasma-membrane-associated, swollen mitochondrion which has expelled material through the plasma membrane. (**G**) A 3D reconstruction of segmentation from a SBF-SEM stack showing normal mitochondria (blue) and narrow mitochondria (green) apparently undergoing fission (white arrows).

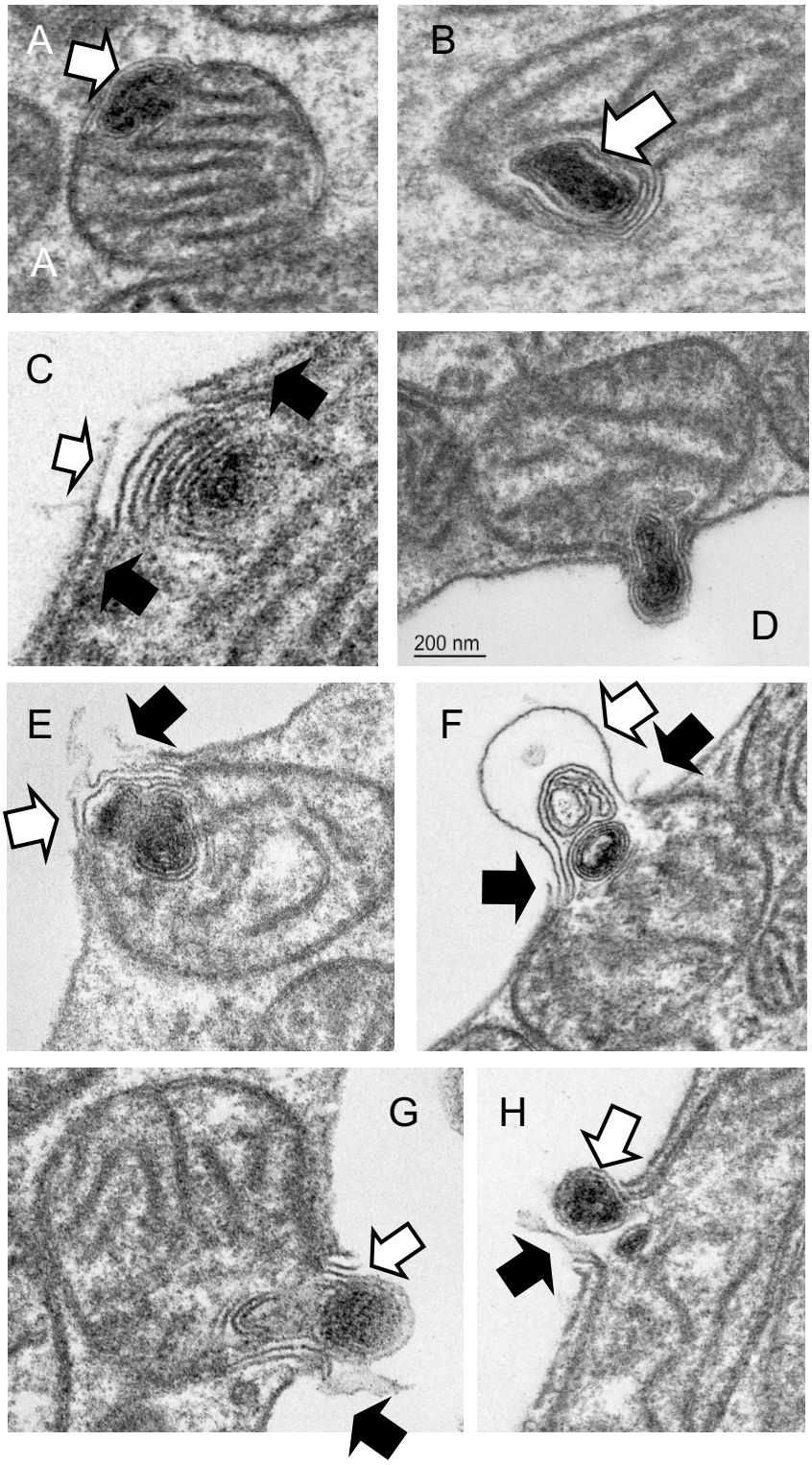

Figure 5. Mitochondria in stressed cones expel electron-dense, membranous contents through the plasma membrane. (**A**,**B**) Electron dense membranous aggregates in mitochondria are associated with electron-lucent domains of the mitochondrion inter-membrane space (white arrows). (**C**–**H**) Mitochondria engage with the plasma membrane, undergo a series of membrane fusions and eject the membranous aggregate into the inter photoreceptor space. (White arrows: swollen or ruptured mitochondrial outer membrane, black arrows: ruptured plasma membrane.

In cones exhibiting heterogeneous mitochondria we also observed regions of elongated, narrow mitochondria in which we could identify sites of possible mitochondrial fission (Fig. 4G).

Mitochondria in stressed rod photoreceptors. We identified regions of apparent rod photoreceptor stress where nearby cones often appeared healthy. Apparently stressed rods appeared slightly shrivelled but with normocytic nuclei and extended, normal-looking outer-segments (data not shown). In cross-section, they exhibited swollen mitochondria with electron lucent matrix and few cristae surrounding what appear to be a core of narrow, dense, mitochondria associated with the ciliary rootlet (Fig. 6A–C). In transverse sections it is apparent that these are in fact tadpole-shaped mitochondria composed of swollen domains with few cristae connected to elongated tubular extensions (Fig. 6D). The cristae of these narrow domains partially align with the repeats of the ciliary rootlet (Fig. 6E). Examination of the distance of the mitochondrion from the geographical centre of the cell and an examination of size reveal that in healthy-looking rods rootlet-associated mitochondria tend to be in the core of the photoreceptor and are slightly narrower than those at the cortex of the cells. In stressed cells those that are associated with the rootlet exhibit a narrow profile, whilst those excluded from the rootlet are swollen (Fig. 6F).

In these rods we observed swollen mitochondria containing membranous whorls. These were less dense than those seen in cones, often comprising just a few invaginations. Neck-like connections to the mitochondrial inter membrane space (MIM) were occasionally visible (Fig. 7A). The MIM in this region appeared electron-lucent and depleted, but unlike cones, the mitochondrial membranes in the vicinity of the aggregate are often reduced to a single membrane. In most cases the outer membrane is missing, in others the inner one is absent. Mitochondria with these denuded regions are often visible in the cytoplasm, not only in association with the plasma membrane. When these single-membrane domains contact either the plasma membrane (Fig. 7B–D) or another swollen mitochondrion, we see evidence of a series of membrane fusions resulting in material being ejected from the cell (Fig. 7E) or being exchanged between mitochondria (Fig. 7F).

In some regions we identified what appear to be patches of more extensive retinal stress where stressed/degenerating rods with polymorphic mitochondria were interspersed between apparently healthy rods and cones (Fig. 8A). The nuclei and outer segments of these rods appeared normal (data not shown), suggesting that the cells were still alive if not functional. In these regions the rod inner-segments contained little cytoplasm and were tightly packed with abnormal mitochondria containing electron-dense membranous aggregates (Fig. 8B). Rod mitochondria in neighbouring, healthy-looking cells were narrow and elongated (Fig. 8C). Only a few such mitochondria remain in some cells, and those we saw were restricted to the core of the cell. In the most extreme cases of degeneration the mitochondria appeared bowl-shaped, were closely opposed to the plasma membrane and had a characteristic open-mouthed appearance from which electron-dense material was seen to spew out of the cell (Fig. 8D–F). Expelled material is fibrous or membranous and of varying density, suggesting it unfolds or disperses as it exits. It hung in the inter-photoreceptor space; presumably associated with the inter-photoreceptor matrix (Fig. 8B).

Discussion

In this paper we describe how mitochondrial populations in aging primate photoreceptors preserve crista-rich mitochondrial domains by linking them to the ciliary rootlet whilst aggregated mitochondrial components are expelled from stressed photoreceptors through the plasma membrane.

Using TEM and SBF-SEM to reveal 3D structures we identified a diverse range of mitochondrial forms in healthy-looking and apparently stressed photoreceptors. In healthy-looking cones we see an apical-distal asymmetry in mitochondrial shape with those most distal, closest to the photoreceptor outer segment, being of larger diameter. This suggests that even within the ellipsoid of a healthy cone the mitochondria are not identical. There may be polarisation of fission–fusion along the apical-distal axis.

In rods and cones cortical mitochondria are closely associated with the plasma membrane and are tubular, elongated and narrow. Away from this zone the inner mitochondria are shorter and a little broader. The closeness and extent of the association of the cortical mitochondria with the plasma membrane suggests that some kind of contact site is formed between the mitochondrion outer membrane and the plasma membrane. This may be of the form identified in mouse rod photoreceptors[26]. We identified little evidence of the trans-cellular mitochondrial alignment described in mouse, the photoreceptors being mostly too far apart to allow apposition of such membranes. The photoreceptors are much less tightly packed together in primate retinae than those of rodents in the vicinity of the ellipsoid, with significant inter-photoreceptor matrix between them, making apposition improbable (Supplementary Fig. 1).

We identified thin, tubular subdomains of a sub-population of mitochondria associated with the ciliary rootlets of both rods and cones. These domains have a dense matrix, are free of membranous aggregates and contain abundant, closely-packed cristae. Mitochondria have been shown to associate with rootlets in the photoreceptors of the cow[23] and owl monkey[22] where there is evidence of correlation between the arrangement of cristae and the rootlet striations, something we also observe here. This is indicative of a cross-link between the rootlet and the mitochondrial contact site and cristae organising system (MICOS). We have seen similar results in rabbit photoreceptors (Supplementary Fig. 2) but not in mice or zebrafish (data not shown).

In mammals mitochondrial fission is regulated by dynamin-related protein (Drp1) and its adaptors Fis1, Mff and Mief1[13,16,27]. Drp1 causes fission by encircling the mitochondrion and forming a constriction site as a result of its GTPase activity[28]. Dynamin-related mitochondrial fission proteins such as Drp1 have evolved to polymerise around mitochondria of a particular diameter[29]. If, due to swelling, the mitochondrion has too great a circumference, there would be reduced opportunity for fission events.

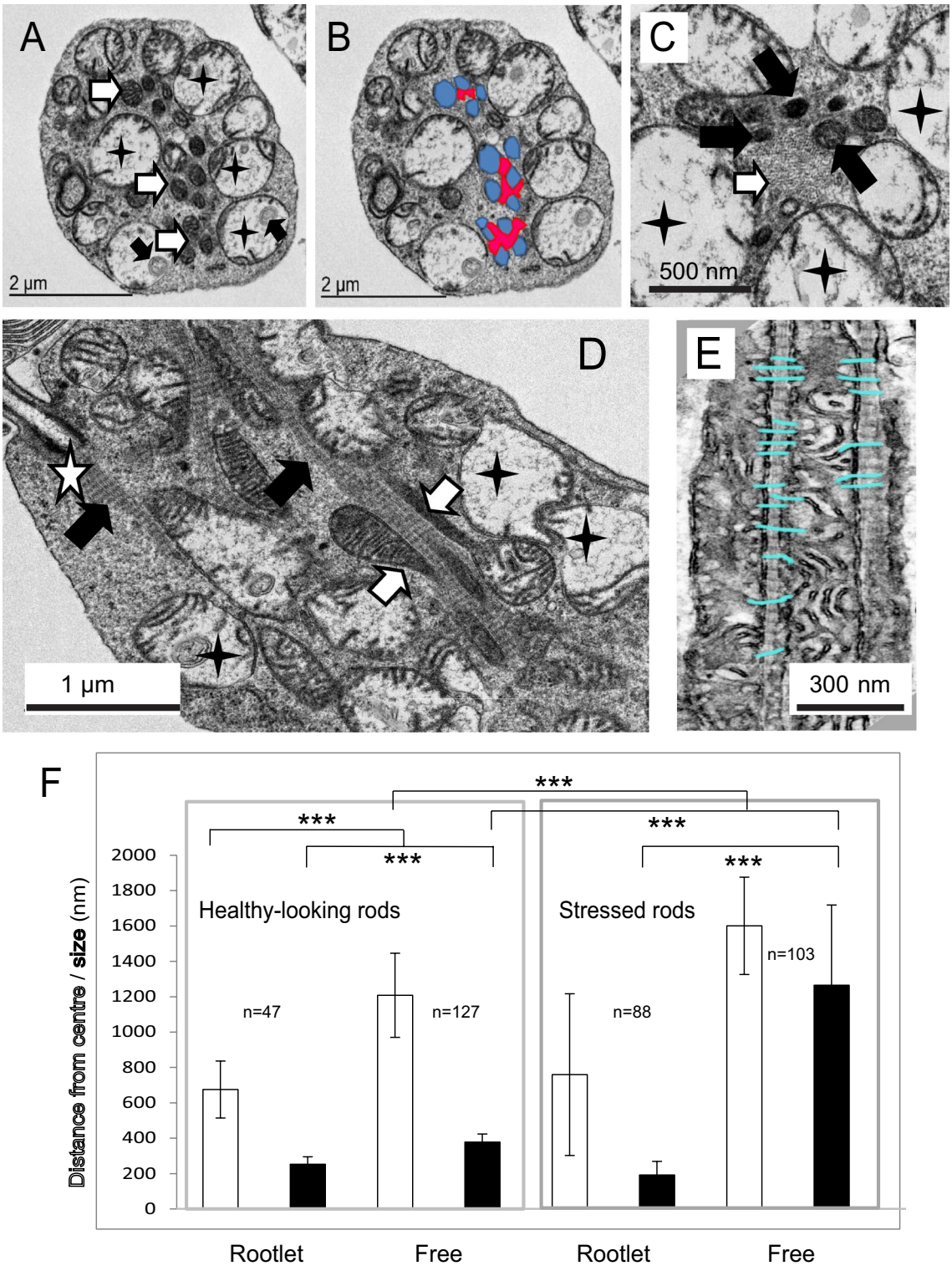

Figure 6. Mitochondria in stressed rods. (**A**) TEM of a transverse section through a stressed rod showing swollen mitochondria with few cristae (black stars). Note the membranous inclusions (black arrows). Narrow, healthy-looking, dense, cristae-rich mitochondria are associated with the rootlet (white arrows). (**B**,**C**) Close up of the rootlet which appears as a fibrous matrix (white arrow), dense mitochondria (black arrows) swollen mitochondria (black stars). (**D**) Longitudinal section of the rod showing mitochondrial extensions (white arrows) aligned with the rootlet (black arrows). The white star indicates the ciliary basal body. (**E**) Mitochondria cristae aligning with the rootletin repeats on the ciliary rootlet. (**F**) Histogram showing the width (size) and distance from the centre of the photoreceptor of rootlet-associated (Rootlet) and non-rootlet-associated (Free) mitochondria in healthy-looking and stressed rods.

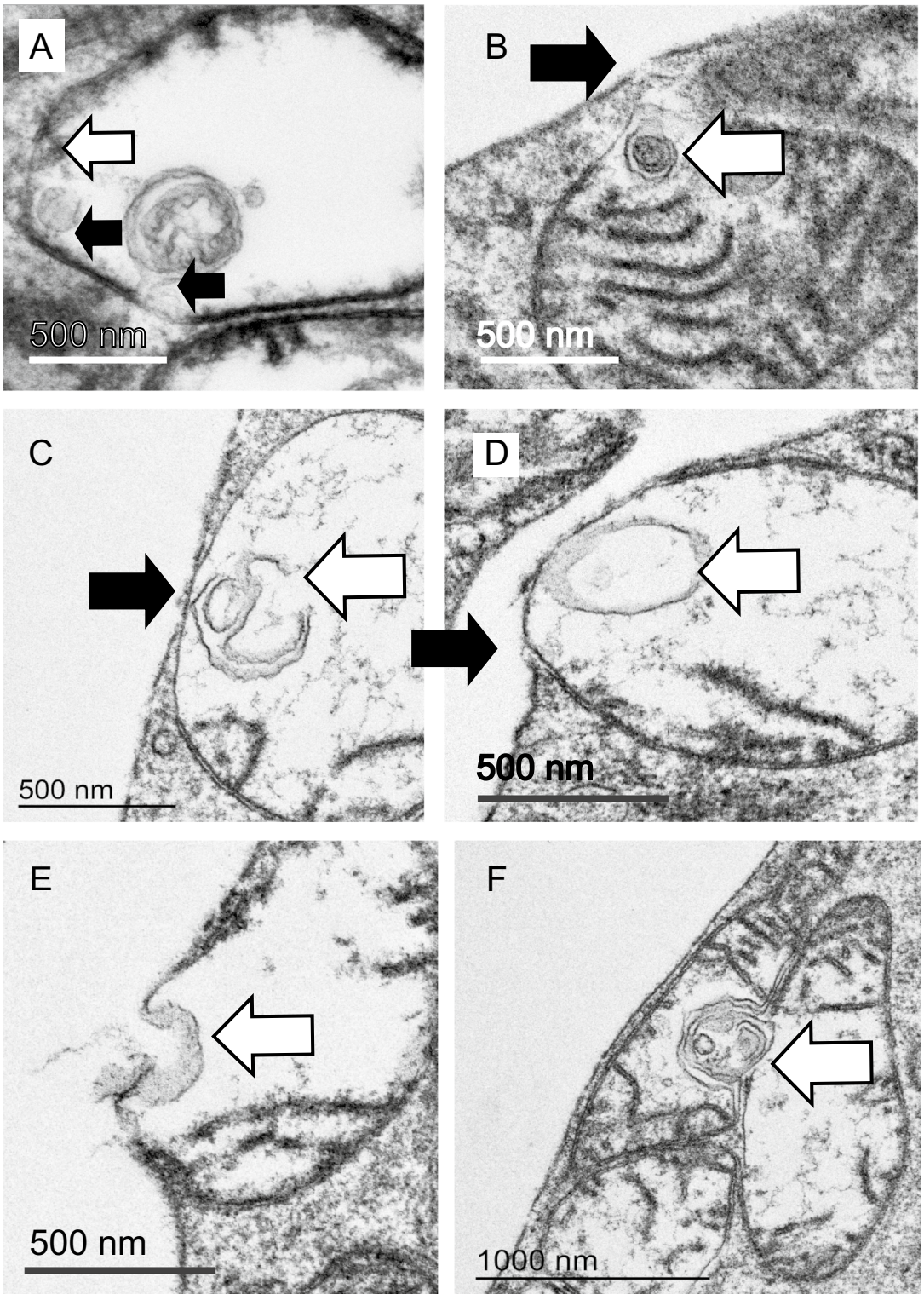

Figure 7. Mitochondria in stressed rods expel and exchange material. (**A**) Swollen mitochondrion in a rod showing few cristae and several internal membranous aggregates connected (presumed) to the inner mitochondrial membrane by a thin 'neck'(black arrows). Note the mitochondrial outer membrane is ruptured in this domain (white arrow). (**B**–**D**) The ruptured mitochondrial membrane engaged with the plasma membrane of the photoreceptor (white arrow: membrane aggregate, black arrow: tear in plasma membrane). (**E**) Multiple membrane fusions result in expulsion of contents. (**F**) Fusion may occur between mitochondria resulting in exchange of membranous contents (white arrow) and possible mitochondrial fusion.

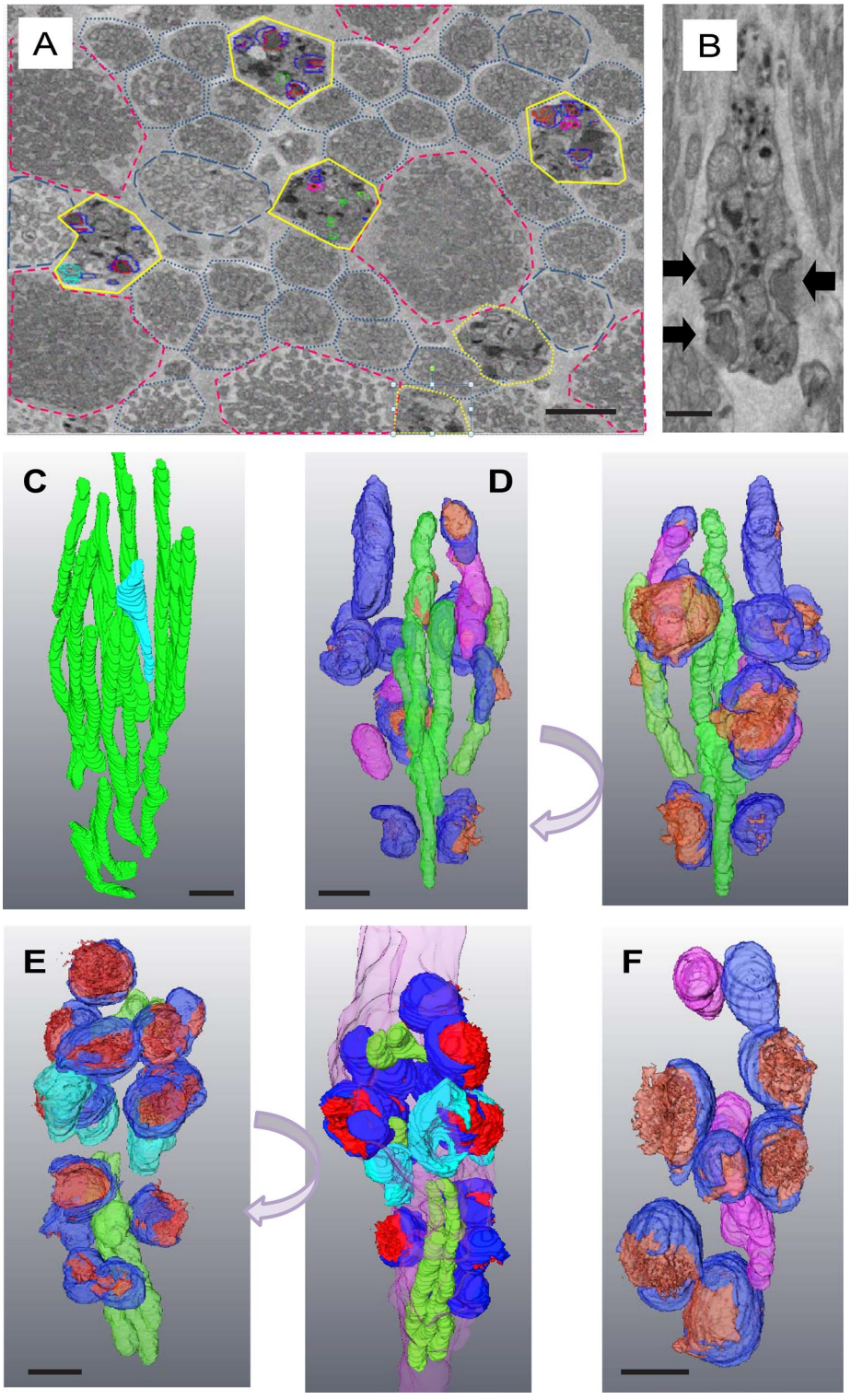

Figure 8. Late stage of degenerating primate rods. (**A**) Low magnification SBF-SEM section of a cluster of late-stage stressed/degenerating rods (high-lighted in yellow). Healthy-looking rods are outlined with blue dots, those containing some swollen mitochondria with blue dashes. Apparently healthy cones are outlined with red dashes. (**B**) Single transverse SBF-SEM section through a late-stage stressed rod. Black arrows indicate electron-dense material being expelled from the mitochondria through the plasma membrane of the photoreceptor. (**C**) Partial segmentation of mitochondria from a healthy-looking rod. The one pale blue mitochondrion shows some swelling. (**B**) Rotations of a rod demonstrating degeneracy. (**D**–**F**) Rotations 3D reconstructions of segmented mitochondria from rods in various late stages of degeneration. (Green: crista-rich elongated, dense mitochondria, magenta: Swollen mitochondria with electron-lucent matrices, dark blue: mitochondria associated with the plasma membrane expelling electron dense contents (red), cyan: mitochondria associated with the plasma membranes that have ejected all their contents. Scale bars 500 nm.

Mechanical force per se is sufficient to recruit the integral mitochondrial fission factor Mff to sites of mitochondrial narrowing[30,31]. This, in turn, recruits Drp1 and results in successful fission[32]. Binding to the rootlet presumably facilitates generation of a force which promotes elongation of the mitochondrion into a thin tubule which may be sufficient to recruit Mff and initiate fission. We were able to identify sites along mitochondrial tubules where they were pinched into narrow necks: these may be the sites of fission. We have also noted that in large, healthy-looking cones the core of the photoreceptor, which is where the rootlet is usually to be found, is populated with small, spherical mitochondrial fragments which are likely to be the products of this fission.

Collectively, this suggests an apical-distal, cortical-core asymmetry of mitochondrial dynamics within single photoreceptor cells in the primate.

Swollen mitochondrial domains with few cristae and individual swollen mitochondria are excluded from the rootlet. We observe invagination of domains of their inner membrane, resulting in formation of electron-dense aggregates in the case of cones, and more diffuse membranous structures in the case of rods. If these aggregates are small, in both rods and cones, they are fully internal to the outer mitochondrial membrane. This excludes the possibility the material is cytoplasmic or lysosomal in origin.

We observe modification or depletion of the mitochondrial outer membrane in the vicinity of electron-dense membranous aggregates which seems to render it susceptible to fusion with the plasma membrane and with other modified domains on other swollen mitochondria. This may result in the release of material from the cell into the inter-photoreceptor space or promote aggregation and fusion of damaged mitochondria. Using 3D electron tomography, we observed what we assume to be highly-stressed rods with very few normal mitochondria, but large, swollen mitochondria attached to the plasma membrane in the process of expelling electron-dense contents out of the cell. Any normal mitochondria present were situated in the core of the inner segment; presumably still associated with the rootlet. In cells undergoing mitochondrial remodelling, the nuclei appear normal and the outer-segment is still intact (data not shown). This implies that the cells are not dead and could potentially still be functional. The changes in mitochondrial form and integrity suggest that cytochrome c may have been released, though in some mouse model systems of apoptosis in photoreceptors mitochondrial cytochrome c release does not occur[33]. We may be observing a very early stage of cell death, or photoreceptors may be refractory to this classical pathway.

Our observations of mitochondrial expulsion of electron-dense aggregates from the photoreceptor are broadly in agreement with those described in zebrafish[34]. In this elegant paper the authors refer to similar structures they identified in mouse. The authors did not mention association of mitochondria with the ciliary rootlet in fish or mice and we have not observed this association in 5 day larval zebrafish or mice retinae (data not shown); although we have identified it in rabbit retinae. Thus, there are differences between fish, mouse, rabbit and primate. It will be interesting to see if elements of rootlet sequestration and trans-plasma membrane expulsion are conserved in human photoreceptors.

Piecemeal mitochondrial degradation, characterised by the production of mitochondrial derived vesicles (MDVs) has been described as a mechanism to isolate damaged material (lipid, protein and mitDNA) from mitochondria and thus purify them[35,36]. The damaged material has been shown to fuse with a subset of peroxisomes[37] or components of the late endosomal pathway such as multivesicular bodies or lysosomes[38] where it can be disposed of or recycled. MDV production occurs during early stages of ROS-induced damage. If damage progresses to a point at which the mitochondria is completely depolarised, redundant or irreparably damaged, it can also be eradicated by a form of autophagy known as mitophagy[39]. This is a slower process that is initiated by components that induce MDV formation; but which then recruits the autophagy machine[40,41]. Conventional piecemeal MDV recycling and mitophagy, superficially at least, appear to be quite distinct from the process we have identified in primate photoreceptors. Our examination of aging or dying photoreceptors in the primate did not reveal the presence of autophagosomes or accumulations of large numbers of multivesicular bodies or lysosomes (our unpublished observations).

Primate rods appear to be more susceptible to photo-damage than cones[42] and are lost in an age-dependent manner leaving cones in a less dense photoreceptor matrix, which is not the case in mice where cones die before rods[43]. In agreement with this, we see far less dramatic changes in mitochondria in cones, though we do see some occasions of mitochondrial tubule formation on the surface of rootlets and can easily identify expulsion of mitochondrial contents from a minority of mitochondria in most cones. In the absence of comparable data from younger, diseased or experimentally stressed individuals, we cannot conclusively state that our observations of 'abnormal' swollen mitochondria are associated with age, stress or degeneration of the photoreceptors; though this seems likely given the maturity of the individuals in this study.

Speculations on the fate of mitochondrial material expelled the photoreceptors. Our observations led us to consider the fate of the material purged from the swollen mitochondria which is likely to be rich in oxidised mitochondrial lipids and mitochondrial proteins. The mitochondrial debris is ultimately likely to be phagocytosed by the retinal pigmented epithelium[44] along with a portion of the outer segment. If this material were generated in significant quantity, as it appears to be in some of the examples we identified, it could overwhelm the RPE or interfere with normal outer-segment phagocytosis and end up being secreted basally, contributing to the basal lateral deposits and drusen (fatty, bleb-like deposits) associated with aging and AMD.

The protein composition of druse provides circumstantial evidence that this might be the case. Drusen are enriched in proteins that have undergone oxidation. Mitochondrial cytochrome c oxidase subunit 5B, mitochondrial aldehyde dehydrogenase and 2-oxoglutarate carrier protein are elevated in basolaminar deposits[45] and the mitochondrial inner membrane protein ATP synthase F1 subunit ATP5B is a common and abundant component of drusen[46]. Cardiolipin, the characteristic phospholipid of mitochondria, has the capacity to initiate the classical complement cascade, remnant deposits of which make up some of the protein contribution to

drusen[47,48]. Cardiolipin also binds to complement factor H (CFH)[49], polymorphisms in which are associated with age-related macular degeneration. Mitochondrial detritus expelled from photoreceptors in the atypical manner described, could not only contribute to basolaminar deposits or drusen, but initiate an unproductive complement response. This provides an alternative source of some of the lipids which make up the bulk of drusen[50] and other age-related lipid deposits.

Received: 3 June 2021; Accepted: 17 August 2021
Published online: 22 September 2021

References

1. Linsenmeier, R. A. Effects of light and darkness on oxygen distribution and consumption in the cat retina. *J. Gen. Physiol.* https://doi.org/10.1085/jgp.88.4.521 (1986).
2. Okawa, H., Sampath, A. P., Laughlin, S. B. & Fain, G. L. ATP consumption by mammalian rod photoreceptors in darkness and in light. *Curr. Biol.* https://doi.org/10.1016/j.cub.2008.10.029 (2008).
3. Kimble, E. A., Svoboda, R. A. & Ostroy, S. E. Oxygen consumption and ATP changes of the vertebrate photoreceptor. *Exp. Eye Res.* https://doi.org/10.1016/S0014-4835(80)80037-6 (1980).
4. Ames, A., Li, Y. Y., Heher, E. C. & Kimble, C. R. Energy metabolism of rabbit retina as related to function: High cost of Na+ transport. *J. Neurosci.* https://doi.org/10.1523/jneurosci.12-03-00840.1992 (1992).
5. Wang, L., Kondo, M. & Bill, A. Glucose metabolism in cat outer retina: Effects of light and hyperoxia. *Investig. Ophthalmol. Vis. Sci.* **38**, 48–55 (1997).
6. Labbé, K., Murley, A. & Nunnari, J. Determinants and functions of mitochondrial behavior. *Annu. Rev. Cell Dev. Biol.* https://doi.org/10.1146/annurev-cellbio-101011-155756 (2014).
7. Noell, W. K. Possible mechanisms of photoreceptor damage by light in mammalian eyes. *Vis. Res.* https://doi.org/10.1016/0042-6989(80)90055-3 (1980).
8. Wright, A. F., Chakarova, C. F., Abd El-Aziz, M. M. & Bhattacharya, S. S. Photoreceptor degeneration: Genetic and mechanistic dissection of a complex trait. *Nat. Rev. Genet.* https://doi.org/10.1038/nrg2717 (2010).
9. Power, M. *et al.* Cellular mechanisms of hereditary photoreceptor degeneration—Focus on cGMP. *Prog. Retin. Eye Res.* https://doi.org/10.1016/j.preteyeres.2019.07.005 (2020).
10 Curcio, C. A., Millican, C. L., Allen, K. A. & Kalina, R. E. Aging of the human photoreceptor mosaic: Evidence for selective vulnerability of rods in central retina. *Investig. Ophthalmol. Vis. Sci.* **34**, 3278–3296 (1993).
11. Otsuga, D. *et al.* The dynamin-related GTPase, Dnm1p, controls mitochondrial morphology in yeast. *J. Cell Biol.* https://doi.org/10.1083/jcb.143.2.333 (1998).
12. Zemirli, N., Morel, E. & Molino, D. Mitochondrial dynamics in basal and stressful conditions. *Int. J. Mol. Sci.* https://doi.org/10.3390/ijms19020564 (2018).
13. Chan, D. C. Mitochondria: Dynamic organelles in disease, aging, and development. *Cell* https://doi.org/10.1016/j.cell.2006.06.010 (2006).
14. Hoppins, S., Lackner, L. & Nunnari, J. The machines that divide and fuse mitochondria. *Annu. Rev. Biochem.* https://doi.org/10.1146/annurev.biochem.76.071905.090048 (2007).
15. Lackner, L. L. & Nunnari, J. M. The molecular mechanism and cellular functions of mitochondrial division. *Biochim. Biophys. Acta Mol. Basis Dis.* https://doi.org/10.1016/j.bbadis.2008.11.011 (2009).
16. Scott, I. & Youle, R. J. Mitochondrial fission and fusion. *Essays Biochem.* https://doi.org/10.1042/BSE0470085 (2010).
17. Eisner, V., Picard, M. & Hajnóczky, G. Mitochondrial dynamics in adaptive and maladaptive cellular stress responses. *Nat. Cell Biol.* https://doi.org/10.1038/s41556-018-0133-0 (2018).
18. Yu, S. B. & Pekkurnaz, G. Mechanisms orchestrating mitochondrial dynamics for energy homeostasis. *J. Mol. Biol.* https://doi.org/10.1016/j.jmb.2018.07.027 (2018).
19. Shutt, T. E. & McBride, H. M. Staying cool in difficult times: Mitochondrial dynamics, quality control and the stress response. *Biochim. Biophys. Acta Mol. Cell Res.* https://doi.org/10.1016/j.bbamcr.2012.05.024 (2013).
20. Yang, J. *et al.* Rootletin, a novel coiled-coil protein, is a structural component of the ciliary rootlet. *J. Cell Biol.* https://doi.org/10.1083/jcb.200207153 (2002).
21. Yang, J. *et al.* The ciliary rootlet maintains long-term stability of sensory cilia. *Mol. Cell. Biol.* https://doi.org/10.1128/mcb.25.10.4129-4137.2005 (2005).
22. Murray, R. G., Jones, A. E. & Murray, A. Fine structure of photoreceptors in the owl monkey. *Anat. Rec.* https://doi.org/10.1002/ar.1091750404 (1973).
23. Wolfrum, U. Cytoskeletal elements in arthorpod sensilla and mammalian photoreceptors. *Biol. Cell* https://doi.org/10.1016/0248-4900(92)90441-3 (1992).
24. Kam, J. H. *et al.* Fundamental differences in patterns of retinal ageing between primates and mice. *Sci. Rep.* **9**, 1–14 (2019).
25. Walton, J. Lead aspartate, an en bloc contrast stain particularly useful for ultrastructural enzymology. *J. Histochem. Cytochem. Off. J. Histochem. Soc.* **27**, 1337–1342 (1979).
26. Meschede, I. P. *et al.* Symmetric arrangement of mitochondria: Plasma membrane contacts between adjacent photoreceptor cells regulated by opa1. *Proc. Natl. Acad. Sci. U. S. A.* https://doi.org/10.1073/pnas.2000304117 (2020).
27. Otera, H. *et al.* Mff is an essential factor for mitochondrial recruitment of Drp1 during mitochondrial fission in mammalian cells. *J. Cell Biol.* https://doi.org/10.1083/jcb.201007152 (2010).
28. Smirnova, E., Griparic, L., Shurland, D. L. & Van der Bliek, A. M. Dynamin-related protein Drp1 is required for mitochondrial division in mammalian cells. *Mol. Biol. Cell* https://doi.org/10.1091/mbc.12.8.2245 (2001).
29. Ingerman, E. *et al.* Dnm1 forms spirals that are structurally tailored to fit mitochondria. *J. Cell Biol.* https://doi.org/10.1083/jcb.200506078 (2005).
30. Gandre-Babbe, S. & Van Der Bliek, A. M. The novel tail-anchored membrane protein Mff controls mitochondrial and peroxisomal fission in mammalian cells. *Mol. Biol. Cell* https://doi.org/10.1091/mbc.E07-12-1287 (2008).
31. Helle, S. C. J. *et al.* Mechanical force induces mitochondrial fission. *Elife* https://doi.org/10.7554/eLife.30292 (2017).
32 Friedman, J. R. *et al.* ER tubules mark sites of mitochondrial division. *Science (80-).* https://doi.org/10.1126/science.1207385 (2011).
33. Doonan, F., Donovan, M. & Cotter, T. G. Caspase-independent photoreceptor apoptosis in mouse models of retinal degeneration. *J. Neurosci.* https://doi.org/10.1523/jneurosci.23-13-05723.2003 (2003).
34. Giarmarco, M. M. *et al.* Daily mitochondrial dynamics in cone photoreceptors. *Proc. Natl. Acad. Sci.* https://doi.org/10.1073/pnas.2007827117 (2020).
35. Soubannier, V. *et al.* A vesicular transport pathway shuttles cargo from mitochondria to lysosomes. *Curr. Biol.* https://doi.org/10.1016/j.cub.2011.11.057 (2012).

36. Sugiura, A., McLelland, G., Fon, E. A. & McBride, H. M. A new pathway for mitochondrial quality control: Mitochondrial-derived vesicles. *EMBO J.* https://doi.org/10.15252/embj.201488104 (2014).
37. Neuspiel, M. *et al.* Cargo-selected transport from the mitochondria to peroxisomes is mediated by vesicular carriers. *Curr. Biol.* https://doi.org/10.1016/j.cub.2007.12.038 (2008).
38. Soubannier, V., Rippstein, P., Kaufman, B. A., Shoubridge, E. A. & McBride, H. M. Reconstitution of mitochondria derived vesicle formation demonstrates selective enrichment of oxidized cargo. *PLoS One* https://doi.org/10.1371/journal.pone.0052830 (2012).
39. Lazarou, M. *et al.* The ubiquitin kinase PINK1 recruits autophagy receptors to induce mitophagy. *Nature* https://doi.org/10.1038/nature14893 (2015).
40. Kanki, T., Wang, K., Cao, Y., Baba, M. & Klionsky, D. J. Atg32 is a mitochondrial protein that confers selectivity during mitophagy. *Dev. Cell* https://doi.org/10.1016/j.devcel.2009.06.014 (2009).
41. Liu, Y. & Okamoto, K. Regulatory mechanisms of mitophagy in yeast. *Biochim Biophys Acta Gen Subj.***1865**(5), 129858. https://doi.org/10.1016/j.bbagen (2021).
42. Okano, K. *et al.* Retinal cone and rod photoreceptor cells exhibit differential susceptibility to light-induced damage. *J. Neurochem.* https://doi.org/10.1111/j.1471-4159.2012.07647.x (2012).
43. Cunea, A. & Jeffery, G. The ageing photoreceptor. *Vis. Neurosci.* https://doi.org/10.1017/S0952523807070204 (2007).
44. Bok, D. The retinal pigment epithelium: A versatile partner in vision. *J. Cell Sci.* https://doi.org/10.1242/jcs.1993.supplement_17.27 (1993).
45. Crabb, J. W. The proteomics of drusen. *Cold Spring Harb. Perspect. Med.* https://doi.org/10.1101/cshperspect.a017194 (2014).
46. Wang, L. *et al.* Abundant lipid and protein components of drusen. *PLoS One* https://doi.org/10.1371/journal.pone.0010329 (2010).
47. Anderson, D. H. *et al.* The pivotal role of the complement system in aging and age-related macular degeneration: Hypothesis revisited. *Prog. Retin. Eye Res.* https://doi.org/10.1016/j.preteyeres.2009.11.003 (2010).
48. Hageman, G. S. *et al.* An integrated hypothesis that considers drusen as biomarkers of immune-mediated processes at the RPE-Bruch's membrane interface in aging and age-related macular degeneration. *Prog. Retin. Eye Res.* https://doi.org/10.1016/S1350-9462(01)00010-6 (2001).
49. Kertesz, Z. *et al.* Characterization of binding at human β2-glycoprotein I to cardiolipin. *Biochem. J.* https://doi.org/10.1042/bj3100315 (1995).
50. Wang, L. *et al.* Lipoprotein particles of intraocular origin in human bruch membrane: An unusual lipid profile. *Investig. Ophthalmol. Vis. Sci.* https://doi.org/10.1167/iovs.08-2376 (2009).

Acknowledgements
We thank Public Health England for their assistance in obtaining the tissues used. We also thank Sandie Holmes from PHE for her invaluable assistance during tissue collection. We would like to thank Professor Tim Levine for comments on the manuscript.

Author contributions
M.J.H. designed and performed the experiments and wrote the manuscript. D.T.W. assisted in data acquisition and provided discussion. J.H.K., M.B.P. and G.J. provided sample material and provided valued discussion. All authors reviewed the manuscript.

Funding
BBSRC BB/N000250/1.

Competing interests
The authors declare no competing interests.

Additional information
Supplementary Information The online version contains supplementary material available at https://doi.org/10.1038/s41598-021-98409-7.

Correspondence and requests for materials should be addressed to M.J.H.

Reprints and permissions information is available at www.nature.com/reprints.

Publisher's note Springer Nature remains neutral with regard to jurisdictional claims in published maps and institutional affiliations.

Open Access This article is licensed under a Creative Commons Attribution 4.0 International License, which permits use, sharing, adaptation, distribution and reproduction in any medium or format, as long as you give appropriate credit to the original author(s) and the source, provide a link to the Creative Commons licence, and indicate if changes were made. The images or other third party material in this article are included in the article's Creative Commons licence, unless indicated otherwise in a credit line to the material. If material is not included in the article's Creative Commons licence and your intended use is not permitted by statutory regulation or exceeds the permitted use, you will need to obtain permission directly from the copyright holder. To view a copy of this licence, visit http://creativecommons.org/licenses/by/4.0/.

© The Author(s) 2021